Protein Delivery

DOI: 10.1002/anie.201410006

Covalent Attachment of Cyclic TAT Peptides to GFP Results in Protein Delivery into Live Cells with Immediate Bioavailability**

Nicole Nischan, Henry D. Herce, Francesco Natale, Nina Bohlke, Nediljko Budisa, M. Cristina Cardoso, and Christian P. R. Hackenberger**

Abstract: *The delivery of free molecules into the cytoplasm and nucleus by using arginine-rich cell-penetrating peptides (CPPs) has been limited to small cargoes, while large cargoes such as proteins are taken up and trapped in endocytic vesicles. Based on recent work, in which we showed that the transduction efficiency of arginine-rich CPPs can be greatly enhanced by cyclization, the aim was to use cyclic CPPs to transport full-length proteins, in this study green fluorescent protein (GFP), into the cytosol of living cells. Cyclic and linear CPP–GFP conjugates were obtained by using azido-functionalized CPPs and an alkyne-functionalized GFP. Our findings reveal that the cyclic-CPP–GFP conjugates are internalized into live cells with immediate bioavailability in the cytosol and the nucleus, whereas linear CPP analogues do not confer GFP transduction. This technology expands the application of cyclic CPPs to the efficient transport of functional full-length proteins into live cells.*

Arginine-rich cell-penetrating peptides (CPPs) have the ability to cross into cells and transport other molecular cargoes in a non-endocytic manner.[1] This mode of cellular delivery, hereafter referred to as transduction, offers immediate free access to the cytoplasm and nucleus, thus making it ideal for the transport of drugs and biomarkers.[2] The transduction efficiency is, however, limited by the size of the cargo,[3] which has confined the application of CPPs to the non-endocytic delivery of small cargoes, such as fluorophores or small to medium-sized peptides. By contrast, proteins coupled to linear CPPs are taken up largely into cytoplasmic vesicles, which leads to endosomal trapping and lysosomal degradation with little or no access to intracellular targets. Great effort has been invested into trying to overcome this barrier and deliver full-length proteins into living cells by using CPPs. Earlier studies reported the delivery of an arginine-rich green fluorescent protein (GFP) fusion, which apparently resulted in free intracellular GFP.[4] However, these results were subsequently shown to be a consequence of fixation artifacts.[5] More recent reports on arginine-substituted supercharged GFP have shown cellular uptake, but the protein was trapped in endocytic vesicles.[6] Alternative approaches for protein delivery include physical disruption of the plasma membrane by electroporation or microinjection and the use of delivery additives.[7] In this study, we employed chemoselective conjugation strategies to attach synthetic CPPs to facilitate passive intracellular protein delivery. This approach minimizes cellular stress and thus holds great potential for pharmaceutical applications. Recently, we discovered that the transduction efficiency of arginine-rich peptides, such as the TAT peptide,[8] can be greatly enhanced by employing cyclic analogues.[9] More specifically, we showed that the cyclization of arginine-rich peptides significantly increases the speed at which these peptides enter living cells. However, it remained an open question whether, besides an increase in kinetic efficiency, cyclization also enables the transport of larger cargoes in a non-endocytic manner, thus overcoming the cargo size limit for transduction.[3] Therefore, we investigated whether this simple structural modification of the peptide enables the transduction of full-length proteins. GFP is a frequently used model protein for probing cellular protein uptake because its intracellular distribution in living cells can be immediately detected by using live-cell confocal microscopy. Moreover, the fluorescence of GFP indicates correct folding of the protein structure. Herein, we show that after conjugating GFP to a cyclic TAT CPP, the protein is delivered into living cells and is immediately free in the cytosol and nucleus.

To access a site-specific cyclic TAT–GFP conjugate (**cTAT-GFP**; Figure 1b), we applied the chemoselective

[*] N. Nischan,[+] Prof. C. P. R. Hackenberger[+]
Leibniz-Institut für Molekulare Pharmakologie (FMP)
Robert-Rössle-Strasse 10, 13125 Berlin (Germany)
E-mail: hackenbe@fmp-berlin.de
N. Nischan[+]
Freie Universität Berlin, Institut für Chemie und Biochemie
Takustrasse 3, 14195 Berlin (Germany)
Dr. H. D. Herce,[+] Dr. F. Natale, Prof. M. C. Cardoso[+]
Technische Universität Darmstadt, Fachbereich Biologie
Schnittspahnstrasse 10, 64287 Darmstadt (Germany)
E-mail: Cardoso@bio.tu-darmstadt.de
Dr. H. D. Herce[+]
Department of Physics, Applied Physics, and Astronomy
Rensselaer Polytechnic Institute
110 Eighth Street, Troy, NY, 12180 (United States)
N. Bohlke, Prof. N. Budisa
Technische Universität Berlin, Institut für Chemie
Müller-Breslau-Str. 10, 10623 Berlin (Germany)
Prof. C. P. R. Hackenberger[+]
Humboldt Universität zu Berlin, Department Chemie
Brook-Taylor-Strasse 2, 12489 Berlin (Germany)
[+] These authors contributed equally.

[**] This work was funded by the Deutsche Forschungsgemeinschaft (SPP1623, Teilprojekt Prof. Cardoso/ Prof. Hackenberger/ Prof. Leonhardt, SFB765 B5), the Fonds der Chemischen Industrie, and the Boehringer-Ingelheim Foundation (Plus 3 award). We also thank Anne Lehmkuhl for excellent technical support.

Supporting information for this article is available on the WWW under http://dx.doi.org/10.1002/anie.201410006.

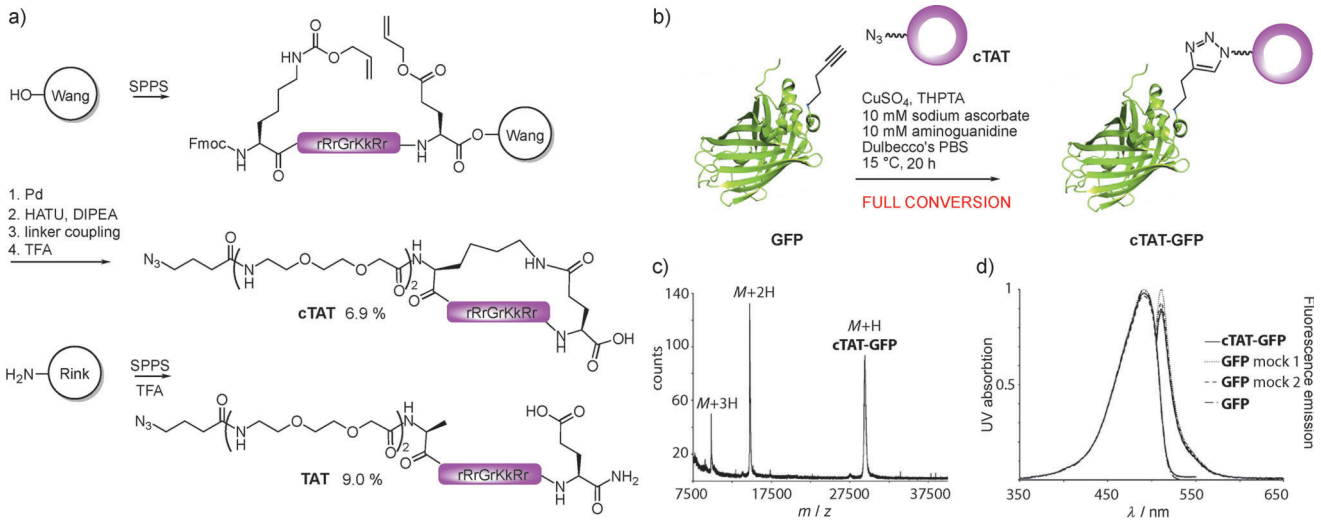

Figure 1. Synthesis of conjugatable cyclic and linear TAT-derived CPPs and conjugation with **GFP**. a) Synthesis of the peptides **cTAT** and **TAT**. b) CuAAC of alkyne-GFP and **cTAT** under optimized conditions to yield **cTAT-GFP**. c) MALDI spectrum of the reaction product after dialysis. d) Absorption and fluorescence emission (excitation at 495 nm) of **cTAT-GFP**, untreated **GFP**, and **GFP** treated with all reagents except azide (**GFP** mock 1) or no reagents (**GFP** mock 2). Each set of graphs was normalized to the graph with the highest intensity.

copper-catalyzed azide–alkyne cycloaddition (CuAAC)[10]. A cyclic azido-TAT peptide (**cTAT**) was reacted with a GFP mutant, obtained through auxotrophic expression in *E. coli*,[11] that carries a homopropargyl glycine at the N terminus (see the Supporting Information). The use of chemoselective protein modification techniques[12] is essential not only for control of the conjugation site but also since cyclic peptides cannot be introduced by standard protein biosynthesis. The cyclic CPP for the later uptake experiments was designed to contain a highly positively charged TAT sequence of alternating L and D amino acids for maximal uptake efficiency[9] and a flexible spacer region carrying the reactive azido group at a reasonable distance to facilitate effective conjugation and flexible presentation of the peptide.

The cyclic TAT peptide was synthesized on a standard Wang resin with orthogonal protecting groups at Lys and Glu for cyclization on the solid support (Figure 1a). Initially, we used a short five amino acid peptide (GKGNG) as a spacer and either azido benzoic acid or azido butanoic acid at the N terminus. The corresponding peptides were obtained in 3–4% overall yield (see the Supporting Information).

However, despite optimization efforts, these CPPs resulted only in incomplete conversions in the later CuAAC conjugation studies (Figures S6, S7 in the Supporting Information). Moreover, the separation of **GFP** and the conjugation product was not successful. However, a cyclic TAT peptide with an N-terminal azide and an oligoethylene glycol spacer (**cTAT**, Figure 1a) could be isolated in spite of its extreme hydrophilicity and in only one purification step through reversed phase HPLC at reduced flow rate in an overall yield of 6.9%. Most importantly, this azido-peptide building block also demonstrated superior results in terms of conjugation to the alkyne-GFP. For the CuAAC, we started with a general method[10c] previously employed for the glycosylation of alkyne-containing proteins in our group[13] and optimized it for the conjugation of **GFP** and **cTAT**. We found that full conversion and good recovery is reached reproducibly at 15 °C in 20 h (Figure 1b,c). Purification of the protein with optimal recovery was achieved by performing dialysis against EDTA in Dulbecco's PBS, followed by HEPES buffer.

As an additional control, we synthesized a linear TAT–GFP conjugate (**TAT-GFP**) through an analogous synthetic strategy to probe the impact of cyclization of the TAT sequence on cellular uptake (see Figure 1a and the Supporting Information). The linear **TAT** peptide is the equivalent of **cTAT** in terms of stereochemistry and linker design; minor changes include an alanine to reflect the cyclized lysine and a glutamic acid with a C-terminal amide instead of a carboxylic acid to maintain overall charge and proteolytic stability of the C terminus. Nonconjugated **GFP** that underwent the same chemical procedures as the CPP-conjugated variants was used as a negative control in the uptake experiments.

To verify that the conjugation has no influence on the photophysical properties of GFP, we compared the UV-absorption and fluorescence spectra (Figure 1d) of isolated **cTAT-GFP** to those of **GFP** protein samples exposed to an identical procedure but either without the azide group (**GFP** mock 1) or with no reagents (**GFP** mock 2), as well as **GFP** that was only subjected to the workup. At similar protein concentrations, all of the tested proteins showed equal absorbance maxima at 495 nm, as well as fluorescence emission maxima at 509 nm with similar intensities (Figure S12–14).

At the outset of our cell uptake studies, we illustrated our desired mode of cellular uptake (transduction) by comparing the uptake of a linear TAT–fluorophore conjugate to that of an amphipathic fluorescently labeled control peptide (PTD4; see the Supporting Information for the conditions).[1a,2a,b] Although both peptides have affinity for the plasma membrane, while the PTD4 gets trapped in endosomes, the TAT-conjugated peptide is successfully delivered into the cell and

can be found freely distributed throughout the cell (Figure S15).

We then compared the cellular uptake and intracellular distribution of **cTAT-GFP**, **TAT-GFP**, and unconjugated **GFP** by performing live-cell confocal microscopy in a human cervical cancer cell line (HeLa). The cells were incubated with the proteins for 40 min in HEPES buffer lacking nutrients and glucose to reduce endocytosis at the concentrations indicated, imaged (Figure S16), and finally washed and imaged again (Figure 2). For quantification of the transduction efficiency, all cells showing homogenous staining of cytoplasm and nucleoli were considered positive. The results show that unconjugated **GFP** at 150 μM was not taken up by living cells (Figure 2a). We also added rhodamine-labeled TAT CPP at 5 μM concentration to the unconjugated **GFP** solution (Figure 2b). While the TAT CPP was taken up into most of the cells and accumulated in the cytosol and nucleolus at high levels, the unconjugated **GFP** at 30-fold higher concentration was not internalized by the cells. Next, we tested the cellular uptake efficiency of the linear **TAT-GFP** conjugate at different concentrations (50, 100 and 150 μM). We detected very low intracellular **GFP** signal, even at the highest concentration used (150 μM); only 1% of the cells were transduced (Figure 2c,e), which is in accordance with our previous observations.[3] No uptake was detected at 50 and 100 μM. By contrast, **cTAT-GFP** was efficiently taken up by most of the living cells at all concentrations tested (50–150 μM; Figure 2d,e). In our earlier observations with cyclic TAT peptide versus linear TAT peptide, we found that the larger arginine side chain separation in cyclic TAT increased the uptake efficiency and kinetics.[9] The data presented herein show that this structural modification can also be exploited for the delivery of much larger cargoes, in this case a fully folded 27.5 kDa protein.

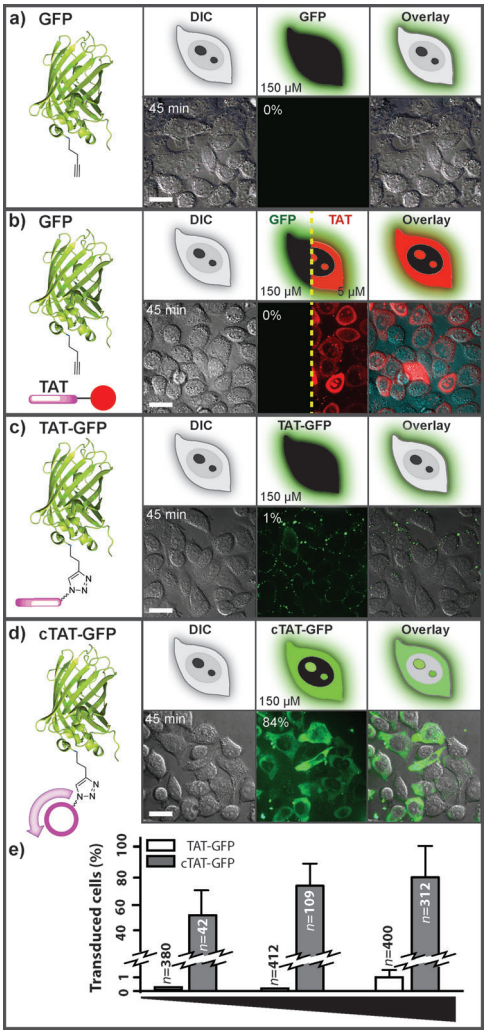

Figure 2. Chemoselective conjugation of **GFP** to cyclic **cTAT** enables the transduction of living cells. a) **GFP** added to the extracellular media was not taken up by living cells. b) While the TAT peptide was able to efficiently enter living cells, unconjugated **GFP** remained excluded from the cells. c) Conjugation of linear **TAT** to **GFP** (**TAT-GFP**) does not lead to efficient transduction; at 150 μM, only 1% of the cells contained **TAT-GFP**. d) **cTAT-GFP** efficiently entered living cells. e) Quantification of the percentage of transduced cells for 50, 100 and 150 μM of **TAT-GFP** and **cTAT-GFP**. Cells were scored as positive when showing a diffuse cytoplasmic and nucleolar fluorescence signal. Error bars: standard deviation. Scale bar: 15 μm.

Notably, as indicated by fluorescence recovery after photobleaching (FRAP) experiments, the protein **cTAT-GFP** was freely distributed throughout the cell cytoplasm and nucleus (Figure S17). In particular, the nuclear localization of **GFP** indicates non-endocytic uptake. To further test this mode of entry, we studied the uptake of **cTAT-GFP** in the presence of a macropinocytosis inhibitor and at 4°C (Figure S18), and the results show that the mode of uptake is energy independent.

Upon comparison of intracellular fluorescence relative to extracellular fluorescence before washing, we found that the intracellular concentration of rhodamine-labeled TAT was much higher than the extracellular concentration, whereas the protein conjugate **cTAT-GFP** showed the opposite relationship (Figure S16b,c). We attribute this observation to the significant size difference between a 2 kDa peptide and a 27.5 kDa protein. An estimate of the GFP intracellular concentration is shown in Figure S19. The general morphology of the cells and the fact that the cells continue to move and undergo mitotic division (movie 1) indicates that **cTAT-GFP** uptake is well tolerated and does not interfere with cell integrity or metabolism.

In summary, we have shown that the chemoselective conjugation of cyclic cell-penetrating peptides to alkyne-GFP gives access to full-length folded GFP conjugates, which are taken up into live cells with immediate cytosolic and nuclear availability. Since the incorporation of alkyne groups into proteins is well established, this technology is generally applicable to the production of other transducing proteins with comparable size. This covalent approach offers multiple strategies to further optimize the transduction efficiency of full-length proteins depending on the particular application, such as the coupling of multiple CPPs to a single protein, the exploration of other CPPs such as cyclic R10,[9] and combination with other protein delivery strategies such as electroporation or the use of delivery additives[7]. While these avenues need to be explored to further increase protein uptake under growth conditions and for therapeutic applica-

tions, our results demonstrate remarkably efficient and direct cytosolic delivery of a folded full-length functional protein covalently coupled to a cyclic arginine-rich peptide. This method opens new venues for the application of proteins, for example, in cell screenings.

Experimental Section

Peptide Synthesis: All peptides were synthesized by using solid-phase peptide synthesis and characterized by HPLC-UV or UPLC-UV, as well as high resolution ESI-MS. For detailed synthesis protocols and analytical data for **cTAT** and **TAT**, see the Supporting Information. Details on **TAT-FITC**, **TAT-TAMRA**, and **PTD4-TAMRA** peptides can be found in Ref. [9].

Expression and Purification of HPG-GFP: The plasmid pET30b GFPhs1-RM, which encodes a mutated variant of GFP containing only the N-terminal methionine (Met; GFPhs1-RM,[14] 245 amino acids, 27.6 kDa) was kindly provided by Soundrarajan Nagasundarapandian from the group of Prof. Sun Gu Lee (Pusan University, South Korea). A Tobacco Etch Virus (TEV) protease recognition site was introduced for removal of the C-terminal His-tag. Glutamine at the N-terminus ensures that the N-terminal Met or homopropargylglycine (HPG) is not cleaved. For expression of GFPhs1-RM TEV, the Met auxotrophic *E. coli* strain B834 (DE3) [B→B834[15]→B834 (DE3)][16] was transformed with pET30b GFPhs1-RM TEV. Expression was carried out under a final HPG concentration of 50 mg mL^{-1}. After cell lysis, HPG-GFP (**GFP**) was immobilized on a Ni-NTA column and cleaved by using TEV protease.

CPP–GFP Conjugation: Mutant **GFP** was conjugated with **cTAT** or **TAT** peptides by using CuAAC. Optimized reaction conditions include shaking with 1,000 turns per minute at 15 °C for 20 h in Ca/Mg-free Dulbecco's phosphate-buffered saline (PBS) at final concentrations of 20 μM protein, 500 μM azidopeptide, 200 μM $CuSO_4$, 1 mM THPTA ligand, and 10 mM aminoguanidine hydrochloride and sodium ascorbate; batch size 500 μL. The reaction was quenched with 50 μL of 5 mM EDTA. The copper was removed through dialysis against 2.5 mM EDTA in Ca/Mg-free Dulbecco's PBS, and then the EDTA was removed through dialysis against HEPES buffer. Full conversion and formation of the product was verified through MALDI-TOF.

Cellular uptake experiments were performed as described elsewhere[9] with minor changes. Briefly, cells were washed twice with Ca^{2+}-free medium (without serum) and the peptides were added. Peptides or (un)conjugated GFP proteins were diluted to different concentrations in a buffer (140 mM NaCl, 2.5 mM KCl, 5 mM HEPES, 5 mM glycine, pH value adjusted with NaOH) and incubated with cells for 60 min at 37 °C in optically proficient glass-bottom multiwell chambers (total sample volumes: 30 μL). Subsequently, the peptide solution was gently exchanged with growth medium and the cells were imaged.

Confocal Microscopy and Image Analysis: Imaging was carried out with an UltraVIEWVoX spinning disc confocal system (Perkin-Elmer, UK). Cells were imaged in a closed live cell microscopy chamber (ACU control, Olympus, Japan) heated to 37 °C, with 5 % CO2 and 60 % air humidity, mounted on a Nikon Ti microscope (Nikon, Japan). Image acquisition was performed with a × 60/1.45 NA Planapochromat oil immersion objective lens. Images were obtained with a cooled 14-bit EMCCD camera (C911-50, CamLink). To visualize the GFP signal, a 488 nm excitation laser and a 521 nm emission filter were used. TAMRA was excited by using a 561 nm laser and the emission was filtered through a 587 nm filter. For transduction efficiency calculations, the cells showing homogenous staining of the cytoplasm and nucleoli were considered positive.

Received: October 12, 2014
Published online: December 17, 2014

Keywords: cell-penetrating peptides · click chemistry · cyclic peptides · live-cell microscopy · protein delivery

[1] a) G. Ter-Avetisyan, G. Tunnemann, D. Nowak, M. Nitschke, A. Herrmann, M. Drab, M. C. Cardoso, *J. Biol. Chem.* **2009**, *284*, 3370 – 3378; b) F. Duchardt, M. Fotin-Mleczek, H. Schwarz, R. Fischer, R. Brock, *Traffic* **2007**, *8*, 848 – 866; c) H. D. Herce, A. E. Garcia, M. C. Cardoso, *J. Am. Chem. Soc.* **2014**, DOI: 10.1021/ja507790z.

[2] a) R. Brock, *Bioconjugate Chem.* **2014**, *25*, 863 – 868; b) S. Futaki, H. Hirose, I. Nakase, *Curr. Pharm. Des.* **2013**, *19*, 2863 – 2868; c) H. D. Herce, W. Deng, J. Helma, H. Leonhardt, M. C. Cardoso, *Nat. Commun.* **2013**, *4*, 2660 – 2667.

[3] G. Tunnemann, R. M. Martin, S. Haupt, C. Patsch, F. Edenhofer, M. C. Cardoso, *Faseb J.* **2006**, *20*, 1775 – 1784.

[4] N. J. Caron, Y. Torrente, G. Camirand, M. Bujold, P. Chapdelaine, K. Leriche, N. Bresolin, J. P. Tremblay, *ASGT Mol. Therapy* **2001**, *3*, 310 – 318.

[5] J. P. Richard, K. Melikov, E. Vives, C. Ramos, B. Verbeure, M. J. Gait, L. V. Chernomordik, B. Lebleu, *J. Biol. Chem.* **2003**, *278*, 585 – 590.

[6] a) S. M. Fuchs, R. T. Raines, *ACS Chem. Biol.* **2007**, *2*, 167 – 170; b) B. R. McNaughton, J. J. Cronican, D. B. Thompson, D. R. Liu, *Proc. Natl. Acad. Sci. USA* **2009**, *106*, 6111 – 6116.

[7] a) K. Inomata, A. Ohno, H. Tochio, S. Isogai, T. Tenno, I. Nakase, T. Takeuchi, S. Futaki, Y. Ito, H. Hiroaki, M. Shirakawa, *Nature* **2009**, *458*, 106 – 109; b) T. Takeuchi, M. Kosuge, A. Tadokoro, Y. Sugiura, M. Nishi, M. Kawata, N. Sakai, S. Matile, S. Futaki, *ACS Chem. Biol.* **2006**, *1*, 299 – 303.

[8] A. D. Frankel, C. O. Pabo, *Cell* **1988**, *55*, 1189 – 1193.

[9] G. Lättig-Tünnemann, M. Prinz, D. Hoffmann, J. Behlke, C. Palm-Apergi, I. Morano, H. D. Herce, M. C. Cardoso, *Nat. Commun.* **2011**, *2*, 453 – 464.

[10] a) C. W. Tornøe, C. Christensen, M. Meldal, *J. Org. Chem.* **2002**, *67*, 3057 – 3064; b) V. V. Rostovtsev, L. G. Green, V. V. Fokin, K. B. Sharpless, *Angew. Chem. Int. Ed.* **2002**, *41*, 2596 – 2599; *Angew. Chem.* **2002**, *114*, 2708 – 2711; c) V. Hong, S. I. Presolski, C. Ma, M. G. Finn, *Angew. Chem. Int. Ed.* **2009**, *48*, 9879 – 9883; *Angew. Chem.* **2009**, *121*, 10063 – 10067; d) B. T. Worrell, J. A. Malik, V. V. Fokin, *Science* **2013**, *340*, 457 – 460.

[11] a) N. Budisa, *Angew. Chem. Int. Ed.* **2004**, *43*, 6426 – 6463; *Angew. Chem.* **2004**, *116*, 6586 – 6624; b) L. Wang, P. G. Schultz, *Angew. Chem. Int. Ed.* **2005**, *44*, 34 – 66; *Angew. Chem.* **2005**, *117*, 34 – 68.

[12] a) K. Lang, J. W. Chin, *ACS Chem. Biol.* **2014**, *9*, 16 – 20; b) C. P. R. Hackenberger, D. Schwarzer, *Angew. Chem. Int. Ed.* **2008**, *47*, 10030 – 10074; *Angew. Chem.* **2008**, *120*, 10182 – 10228; c) D. Schumacher, C. P. R. Hackenberger, *Curr. Opin. Chem. Biol.* **2014**, *22*, 62 – 69.

[13] L. M. Artner, L. Merkel, N. Bohlke, F. Beceren-Braun, C. Weise, J. Dernedde, N. Budisa, C. P. R. Hackenberger, *Chem. Commun.* **2012**, *48*, 522 – 524.

[14] S. Nagasundarapandian, L. Merkel, N. Budisa, R. Govindan, N. Ayyadurai, S. Sriram, H. Yun, S. G. Lee, *ChemBioChem* **2010**, *11*, 2521 – 2524.

[15] W. B. Wood, *J. Mol. Biol.* **1966**, *16*, 118 – 133.

[16] a) F. W. Studier, P. Daegelen, R. E. Lenski, S. Maslov, J. F. Kim, *J. Mol. Biol.* **2009**, *394*, 653 – 680; b) F. W. Studier, B. A. Moffatt, *J. Mol. Biol.* **1986**, *189*, 113 – 130.

